Available online at www.sciencedirect.com
ScienceDirect
Journal of Power Sources 167 (2007) 178–184
JOURNAL OF POWER SOURCES
www.elsevier.com/locate/jpowsour

Effect of Cr doping on the structural, electrochemical properties of $Li[Li_{0.2}Ni_{0.2-x/2}Mn_{0.6-x/2}Cr_x]O_2$ ($x = 0$, 0.02, 0.04, 0.06, 0.08) as cathode materials for lithium secondary batteries

Li Fang Jiao, Ming Zhang, Hua Tang Yuan *, Ming Zhao, Jian Guo, Wei Wang, Xing Di Zhou, Yong Mei Wang

Institute of New Energy Material Chemistry, Nankai University, Tianjin 300071, China

Received 1 August 2006; received in revised form 15 January 2007; accepted 17 January 2007
Available online 2 February 2007

Abstract

Prospective positive-electrode (cathode) materials for a lithium secondary battery, viz., $Li[Li_{0.2}Ni_{0.2-x/2}Mn_{0.6-x/2}Cr_x]O_2$ ($x = 0$, 0.02, 0.04, 0.06, 0.08), were synthesized using a solid-state pyrolysis method. The structural and electrochemical properties were examined by means of X-ray diffraction, cyclic voltammetry, SEM and charge–discharge tests. The results demonstrated that the powders maintain the α-$NaFeO_2$-type layered structure regardless of the chromium content in the range $x \leq 0.08$. The Cr doping of $x = 0.04$ showed improved capacity and rate capability comparing to undoped $Li[Li_{0.2}Ni_{0.2}Mn_{0.6}]O_2$. ac impedance measurement showed that Cr-doped electrode has the lower impedance value during cycling. It is considered that the higher capacity and superior rate capability of Cr-doping samples would be ascribed to the reduced resistance of the electrode during cycling.

Keywords: Lithium-ion battery; Cathode material; Cr-doped; Electrochemical behavior; $Li[Li_{0.2}Ni_{0.2-x/2}Mn_{0.6-x/2}Cr_x]O_2$; Layered

1. Introduction

During the past decade, lithium manganese oxides have been extensively studied as an alternative to $LiCoO_2$, which is the state-of-the-art positive electrode material in commercial lithium ion battery systems, due to the relative lower cost and toxicity of Mn compared to Co [1–9]. The drawback of layered Li–Mn oxides is the capacity decay due to the phase transformation of the layered structure to a spinel structure by Jahn–Teller distortion during charge–discharge cycles [10,11]. To solve this problem, a number of research groups have tried to stabilize the layered structure by introducing a $LiMO_2$ (M = Ni, Co, Cr) phase into the layered Li_2MnO_3 to form a solid solution of mixed transition-metal oxides [12–16]. Among the solid solutions being developed, the layered compounds of $Li[Li_{(1-2x)/3}Ni_xMn_{(2-x)/3}]O_2$ seem to be a very promising candidate as a cathodic material for the new generation of Li-ion batteries due to their thermal stability and good electrochemical performances. Lu and Dahn [8,17] found that $Li[Li_{(1-2x)/3}Ni_xMn_{(2-x)/3}]O_2$ ($x = 1/6$, 1/4, 1/3, 5/12) samples displayed a plateau at about 4.5 V versus lithium metal during the first charge, which was believed to correspond to oxygen loss concomitant with Li extraction. Subsequent to this plateau, the materials can reversibly cycle over 225 mAh g^{-1} between 2.0 and 4.6 V [8]. This means that this compound can be used as a cathode material for high capacity lithium secondary batteries. However, this material has to overcome low rate capability and improve thermal stability for a commercial use.

One approach to improve the electrochemical performance is to substitute a small amount of dopant ion at the transition metal sites. Kim et al. have reported increased electrical conductivity by doping Co in $Li[Li_{(1-2x)/3}Ni_xMn_{(2-x)/3}]O_2$ [18]. However, to the best of our knowledge, no studies on the electrochemical performance of electrode-active materials doped by chromium have been published.

In this study, we employed Cr as an additional dopant to synthesize a series of Cr-doped $Li[Li_{0.2}Ni_{0.2-x/2}Mn_{0.6-x/2}Cr_x]O_2$ ($x = 0$, 0.02, 0.04, 0.06, 0.08) powders. The structural, mor-

* Corresponding author. Tel.: +86 22 23498089; fax: +86 22 23502604.
E-mail address: yuanht@nankai.edu.cn (H.T. Yuan).

0378-7753/$ – see front matter © 2007 Elsevier B.V. All rights reserved.
doi:10.1016/j.jpowsour.2007.01.070

phological and electrochemical performances of $Li[Li_{0.2}Ni_{0.2-x/2}Mn_{0.6-x/2}Cr_x]O_2$ powders were studied in this paper.

2. Experimental

2.1. Synthesis of $Li[Li_{0.2}Ni_{0.2-x/2}Mn_{0.6-x/2}Cr_x]O_2$ ($x = 0$, 0.02, 0.04, 0.06, 0.08) powders

To prepare the $Li[Li_{0.2}Ni_{0.2-x/2}Mn_{0.6-x/2}Cr_x]O_2$ ($x = 0$, 0.02, 0.04, 0.06, 0.08) powders, we used stoichiometric $LiCH_3COO{\cdot}2H_2O$, $Ni(CH_3COO)_2{\cdot}4H_2O$, Mn $(CH_3COO)_2{\cdot}4H_2O$, $Cr(NO_3)_3{\cdot}9H_2O$ as the starting materials. These reagents were mixed and thoroughly ground. The mixtures were heated at 120 °C for 48 h to obtain the precursors. Precursors were thoroughly ground again and calcined at 800 °C for 20 h in air, respectively.

2.2. Measurements

X-ray diffraction measurements of the as-prepared $Li[Li_{0.2}Ni_{0.2-x/2}Mn_{0.6-x/2}Cr_x]O_2$ materials were carried out using X-ray diffraction (D/Max-2500) with Cu Kα radiation at room temperature. Particle morphology of the powders after calcination was observed using a scanning electron microscope (SEM, JSM 6400, JEOL, Japan). The composite positive electrodes were prepared by pressing a mixture of the active materials, conductive material (acetylene black) and binder (PTFE) in a weight ratio of 85/10/5. The Li metal was used as the counter and reference electrodes. The electrolyte was 1M $LiPF_6$ in a 6/3/1 (volume ratio) mixture of dimethyl carbonate (DMC), ethylene carbonate (EC), and di-ethylene carbonate (DEC). The cells were assembled in an argon-filled dried box. Charge–discharge tests were performed between 2.5 and 4.8 V. Cyclic voltammetry experiments were performed by using a CHI660 Electrochemical Workstation at a scan rate of 1 mV s^{-1}. ac impedance measurements were carried out using CHI-604A, the frequency range was 0.001 Hz to 100 kHz. All tests were performed at room temperature.

3. Results and discussion

The XRD patterns of the $Li[Li_{0.2}Ni_{0.2-x/2}Mn_{0.6-x/2}Cr_x]O_2$ ($x = 0$, 0.02, 0.04, 0.06, 0.08) materials are shown in Fig. 1. All of the diffraction peaks could be indexed based on a hexagonal α-$NaFeO_2$ structure with a space group of *R*-3*m*, in which layers of lithium atoms alternate with layers containing mixtures of lithium, nickel, chromium and manganese atoms indicating phase pure and a single-phase layered crystal structure. The peaks between 20° and 25° are caused by superlattice ordering of the Li, Ni, Cr, and Mn in the 3*a* site, indicating a layered structure with Li_2MnO_3 character [18–20]. All peaks are sharp and well defined, suggesting that compounds are generally well crystallized. It implies that the chromium substitution for manganese, nickel in $Li[Li_{0.2}Ni_{0.2-x/2}Mn_{0.6-x/2}Cr_x]O_2$ compounds has not changed the bulk structure of the pristine material.

Table 1 shows the variation in lattice constants, *a* and *c*, and *c*/*a* ratio of $Li[Li_{0.2}Ni_{0.2-x/2}Mn_{0.6-x/2}Cr_x]O_2$ ($x = 0$, 0.02, 0.04, 0.06, 0.08) calculated by the Rietveld refinement from the XRD data. As the Cr content, *x*, increases in $Li[Li_{0.2}Ni_{0.2-x/2}Mn_{0.6-x/2}Cr_x]O_2$, lattice constants a and c decrease. It is likely that the decrease in lattice constants is attributed to the substitution of smaller Cr^{3+}($r_{Cr^{3+}} = 0.615$ Å) ion for Ni^{2+} ($r_{Ni^{2+}} = 0.69$ Å) and Mn^{4+}($r_{Mn^{4+}} = 0.60$ Å) ions. The substitution of manganese and nickel by chromium should result in shrinkage of the unit-cell volume, and the decrease in cell volume should increase the stability of the structure during intercalation and de-intercalation of lithium [21–24].

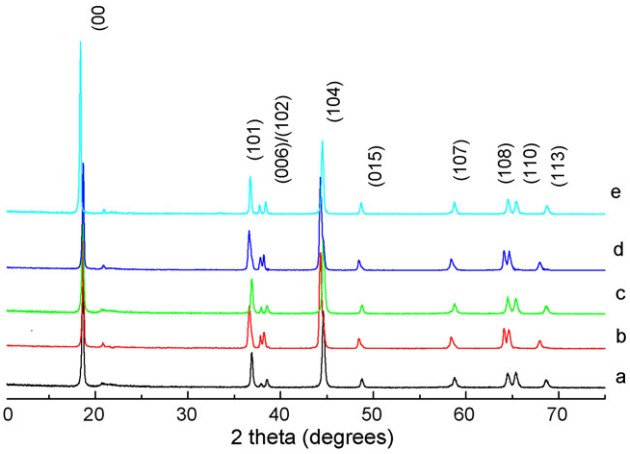

Fig. 1. X-ray diffraction patterns of the $Li[Li_{0.2}Ni_{0.2-x/2}Mn_{0.6-x/2}Cr_x]O_2$ powders: (a) $x = 0$, (b) $x = 0.02$, (c) $x = 0.04$, (d) $x = 0.06$ and (e) $x = 0.08$.

On the other hand, Table 1 also shows that the *c*/*a* ratio increases as *x* value increases. The ratio of *c*/*a* is usually used as the measurement of hexagonality for layered materials. When the ratio is greater than 4.9, it is assumed that the material possesses layered characteristics. Higher amount of Cr substitution for Ni and Mn showed more layer-like structure, which means that good electrochemical performance can be expected.

The particle morphology, particle size and particle size distribution of cathode materials are of great importance to the performance of battery. Cathode materials with small particles tend to have high initial capacity and low cycle stability [25,26]. The uniform particle size distribution leads to the uniform depth of charge (DOC) of each particle, which increases the utilization of the material to enhance the overall battery performance. On the other hand, the smaller particle size means a larger active area to the decomposition of the electrolyte under abnormal abuse conditions such as overcharge or at elevated temperature [27]. So the particle size must be optimized between the performance and safety problems of the batteries. The SEM images of $Li[Li_{0.2}Ni_{0.2-x/2}Mn_{0.6-x/2}Cr_x]O_2$ ($x = 0$,

Table 1
Lattice parameters of the materials in different Cr-doped contents

Samples	*a* (Å)	*c* (Å)	*c*/*a*
$x = 0$	2.8688(6)	14.2595(2)	4.971
$x = 0.02$	2.8642(3)	14.2575(1)	4.978
$x = 0.04$	2.8586(6)	14.2511(3)	4.985
$x = 0.06$	2.8514(2)	14.2452(3)	4.996
$x = 0.08$	2.8483(3)	14.2365(5)	4.998

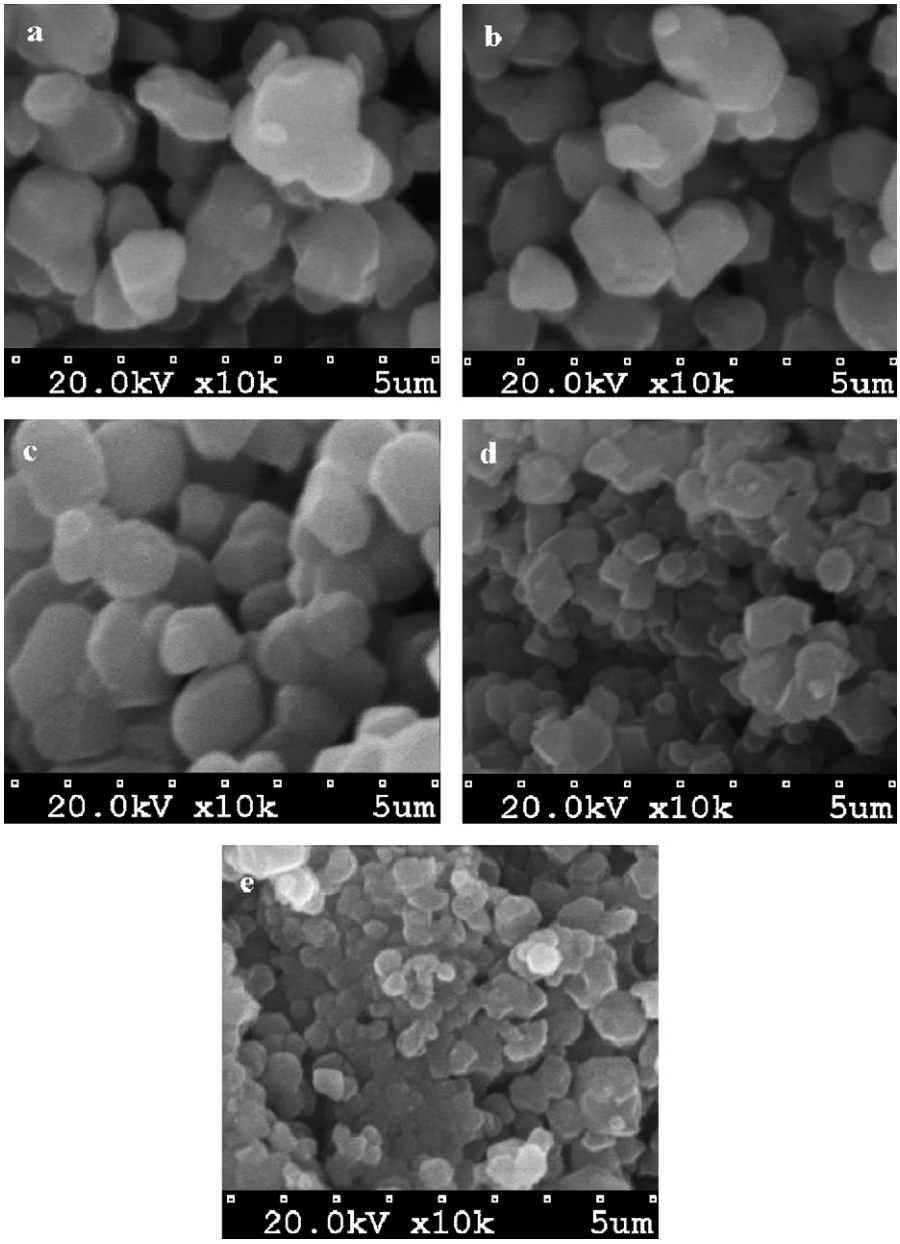

Fig. 2. SEM images of $Li[Li_{0.2}Ni_{0.2-x/2}Mn_{0.6-x/2}Cr_x]O_2$ samples: (a) $x=0$, (b) $x=0.02$, $x=0.04$, (d) $x=0.06$ and (e) $x=0.08$.

0.02, 0.04, 0.06, 0.08) are shown in Fig. 2. The analyses reveal that all powders consist of well-crystallized particles and have the similar morphology. It suggests that Cr is well permeated into the bare $Li[Li_{0.2}Ni_{0.2}Mn_{0.6}]O_2$ forming a solid solution. The average particle size of $Li[Li_{0.2}Ni_{0.2-x/2}Mn_{0.6-x/2}Cr_x]O_2$ with $x=0$ is more than 10 μm. With Cr-doping, the particles shrink slightly due to the smaller ionic radius of Cr^{3+}. On the other hand, It is evident that the presence spherical grains of an independent nature are obtained up to a dopant level of $x=0.04$. The particles of the material with less chromium content exhibit a regular shape with well-developed crystal faces. Slightly agglomerated particles are formed at higher dopant concentrations ($x=0.06$, 0.08), which means the electrochemical capability might descend distinctly [28].

From above discussion, it is believed that the lower Cr doping makes the particle size smaller and more uniform, and produces more independent particles. The features of Cr-doped $Li[Li_{0.2}Ni_{0.2-x/2}Mn_{0.6-x/2}Cr_x]O_2$ with $x=0.02$ and 0.04 powder are very desirable to be employed as electrode-active material for lithium rechargeable battery.

Fig. 3 shows the charge–discharge curves for the $Li[Li_{0.2}Ni_{0.2-x/2}Mn_{0.6-x/2}Cr_x]O_2$ ($x=0$, 0.02, 0.04, 0.06, 0.08) cells between 2.5 and 4.8 V at a current density of 20 mA g^{-1} at room temperature. During the first charge of the cells, The $Li[Li_{0.2}Ni_{0.2}Mn_{0.6}]O_2$ electrodes showed a capacity of ~110 mAh g^{-1} up to about 4.5 V where the slope ends. In this region, the oxidation of Ni ions contributes to the capacity [29]. Above 4. 5 V, all samples showed long plateau, and

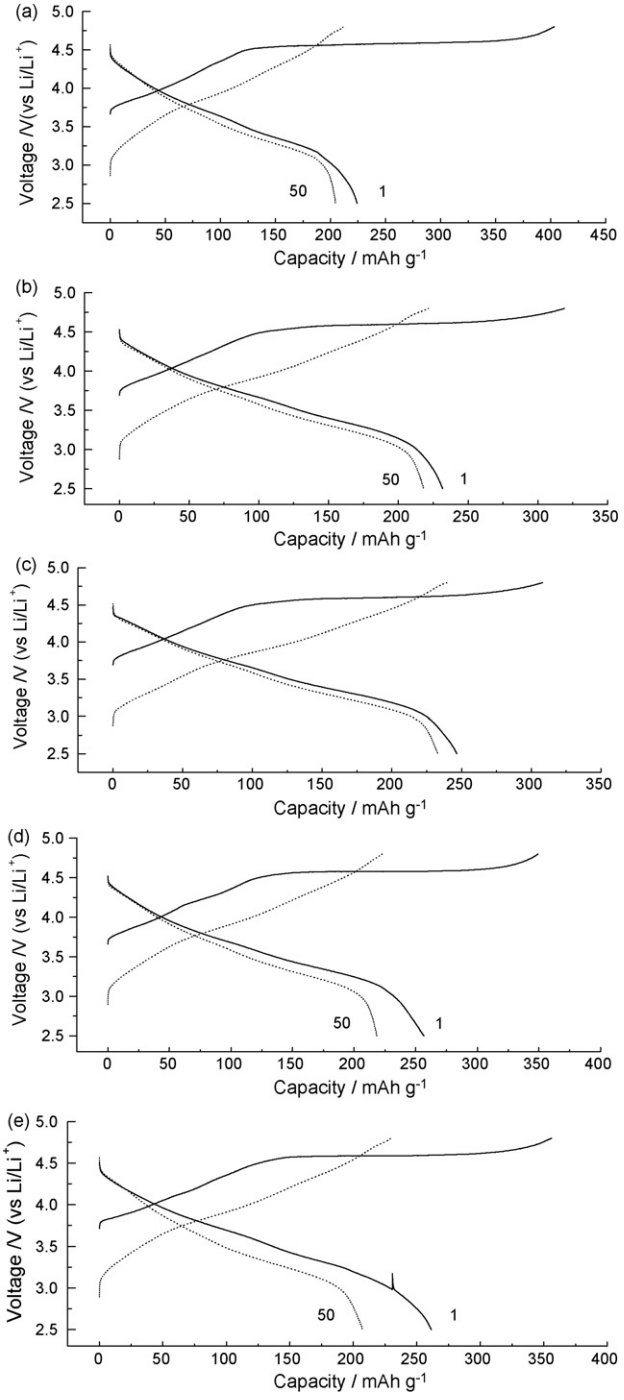

Fig. 3. The charge–discharge curves of $Li[Li_{0.2}Ni_{0.2-x/2}Mn_{0.6-x/2}Cr_x]O_2$ cells at a rate of 20 mA g^{-1} between 2.5 and 4.8 V: (a) $x=0$, (b) $x=0.02$, (c) $x=0.04$, (d) $x=0.06$ and (e) $x=0.08$.

it is irreversible at following cycles. Recent study suggested that the irreversible capacity of the plateau at about 4.5 V is related to the oxygen loss during the first charging [29]. The $Li[Li_{0.2}Ni_{0.2-x/2}Mn_{0.6-x/2}Cr_x]O_2$ electrodes with $x=0$, 0.02, and 0.04 delivered discharge capacities of 225, 232, and 246 mAh g^{-1} initially, and showed excellent capacity retention after 50 cycles. However, the higher level of Cr doping ($x=0.06$, 0.08) led to the capacity fading comparing to the undoped or Cr doped with lower levels ($x=0.02$, 0.04).

A part of charge–discharge data for $Li[Li_{0.2}Ni_{0.2-x/2}Mn_{0.6-x/2}Cr_x]O_2$ materials are provided in Table 2. It can be seen that the initial specific charge capacity decreased and initial specific discharge capacity increased after doping chromium. So the coulombic efficiency of the Cr-doped electrodes was evidently greater than that of pristine material. The highest initial discharge capacity of 261 mAh g^{-1} was obtained by the sample with $x=0.08$. As the chromium doping content decreased from $x=0.06$ to 0.02, the initial discharge capacity decreased from 256 to 232 mAh g^{-1} accordingly. Although the materials with $x=0.08$ and 0.06 cells delivered the higher initial capacity, they showed a rapidly decline within a few number of cycles. For example, the discharge capacity after 50 cycles was 207 mAh g^{-1} with almost 21% loss of capacity for the sample with $x=0.08$ (showed in Table 2). While the samples with $x=0.02$ and 0.04 exhibited slightly lower initial discharge capacity, they had excellent cyclic performance with 7% and 4% loss of capacity after 50 cycles, respectively. Indeed, the $Li[Li_{0.2}Ni_{0.2-x/2}Mn_{0.6-x/2}Cr_x]O_2$ cell with $x=0.04$ gave a discharge capacity of around 235 mAh g^{-1} after 50 cycles, slightly higher than the first discharge capacity of pristine material.

The increase of specific capacity can be attributed to the reason that doping chromium could increase the amount of electrochemical active component in doped materials. Therefore, the new approach of substituting trivalent chromium ions formed a rigid structure, a regular shape with well-developed crystal faces and result in excellent electrochemical performance.

In order to investigate the effect of Cr doping on the rate capability, $Li[Li_{0.2}Ni_{0.2-x/2}Mn_{0.6-x/2}Cr_x]O_2$ ($x=0$, 0.02, 0.04, 0.06, 0.08) cells were cycled between 2.5 and 4.8 V at various current densities in Fig. 4. The cycle life curves for $Li[Li_{0.2}Ni_{0.2-x/2}Mn_{0.6-x/2}Cr_x]O_2$ cathode materials recorded at 0.1 C (20 mA g^{-1}) current rate for one to five cycles, 0.2 C (40 mA g^{-1}) current rate for 6–10 cycles, 0.4 C (80 mA g^{-1}) current rate for 11–15 cycles, 0.8 C (160 mA g^{-1}) current rate for 16–20 cycles, 1.5 C (300 mA g^{-1}) current rate for 21–25 cycles. It can be seen that relatively high discharge capacities of 240–261 mAh g^{-1} were shown at the current den-

Table 2
Charge–discharge data for $Li[Li_{0.2}Ni_{0.2-x/2}Mn_{0.6-x/2}Cr_x]O_2$ cathode materials at a constant current density of 20 mA g^{-1} between 2.5 and 4.8 V at room temperature

Samples	First cycle, $Q_{discharge}$ (mAh g^{-1})	First cycle, $Q_{discharge}$ (mAh g^{-1})	Loss (%)	Fiftieth cycle, $Q_{discharge}$ (mAh g^{-1})	Capacity retention (%)
$x=0$	403	225	44	205	91
$x=0.02$	319	232	27	218	93
$x=0.04$	309	246	21	235	96
$x=0.06$	350	256	27	218	85
$x=0.08$	356	261	26	207	79

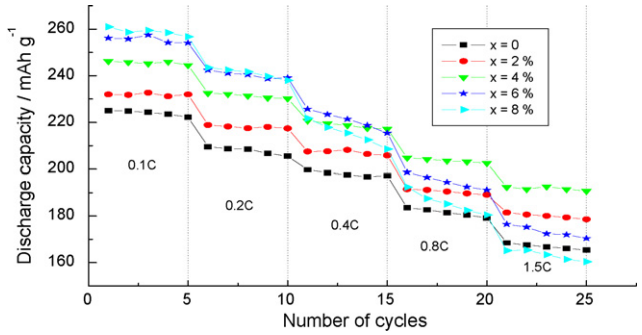

Fig. 4. The capacity retention of undoped and all Cr-doped cells during cycling at various rates in the voltage range of 2.5–4.8 V at room temperature.

sity of 0.1 and 0.2 C for $x = 0.06$, 0.08. By applying higher current density of 0.8 and 1.5 C, the discharge capacities were abruptly decreased, showing fast capacity fading during cycling. On the contrary, the samples with $x = 0.02$ and 0.04 showed higher capacity with improved cyclability at high discharge rate, though they exhibited lower capacity at the current rate of 0.1 and 0.2 C. When the cells were cycled at a current density of 1.5 C, $Li[Li_{0.2}Ni_{0.2-x/2}Mn_{0.6-x/2}Cr_x]O_2$ with $x = 0.04$ cell still exhibited higher discharge capacity of 192 mAh g^{-1}. From this result, we speculated that 4% is the ideal amount of Cr doping for the high-rate capacity of $Li[Li_{0.2}Ni_{0.2-x/2}Mn_{0.6-x/2}Cr_x]O_2$. Recently, Hideyuki Noguchi et al. reported that the a small amount of additional Cr in $LiMn_{0.5-x}Cr_{2x}Ni_{0.5-x}O_2$ can improve the cycling performance but have no positive effects on the rate capability of the sample, they believe the charge transference and lithium ion diffusion during the charge and discharge process are believed to be more factors for the rate capability of the cathode materials [30]. In our study, the cycling performance and rate capability of samples were improved by a small amount of Cr doping. The electrochemical performance of the samples with higher Cr content showed higher discharge capacity and not as good cycling performance because of the structure, which was agreed well with the SEM results in Fig. 2. It can be concluded that the amount of doped chromium can exert significant influence on the structure of these samples which could affect the electrochemical performance. More studies are being processed to investigate the effects of Cr content on the electrochemical performance of layered $Li[Li_{0.2}Ni_{0.2}Mn_{0.6}]O_2$ compound system deeply.

Cyclic voltammetry is a well-suited and complementary technique to evaluate the cathodic performance and electrode kinetics of oxides [31,32]. In order to further understand the effects of Cr doping on the electrochemical properties of $Li[Li_{0.2}Ni_{0.2-x/2}Mn_{0.6-x/2}Cr_x]O_2$, cyclic voltammetry was carried out with Li metal as the counter and reference electrode, in the range 2.5–4.8 V at room temperature, at a scan rate 1 mV s^{-1}. The CV of the typical samples $Li[Li_{0.2}Ni_{0.2-x/2}Mn_{0.6-x/2}Cr_x]O_2$ ($x = 0$, 0.04, 0.08) up to 30 cycles are shown in Fig. 5.

As shown, for $Li[Li_{0.2}Ni_{0.2-x/2}Mn_{0.6-x/2}Cr_x]O_2$ with $x = 0$ and 0.04, there is an appearance of one anodic peak centered at about 4.3 V on charge process, and corresponding reduction peak is seen at 3.8 V on discharge. According to the previous assignments of the CV features [8,16], the anodic peak at about

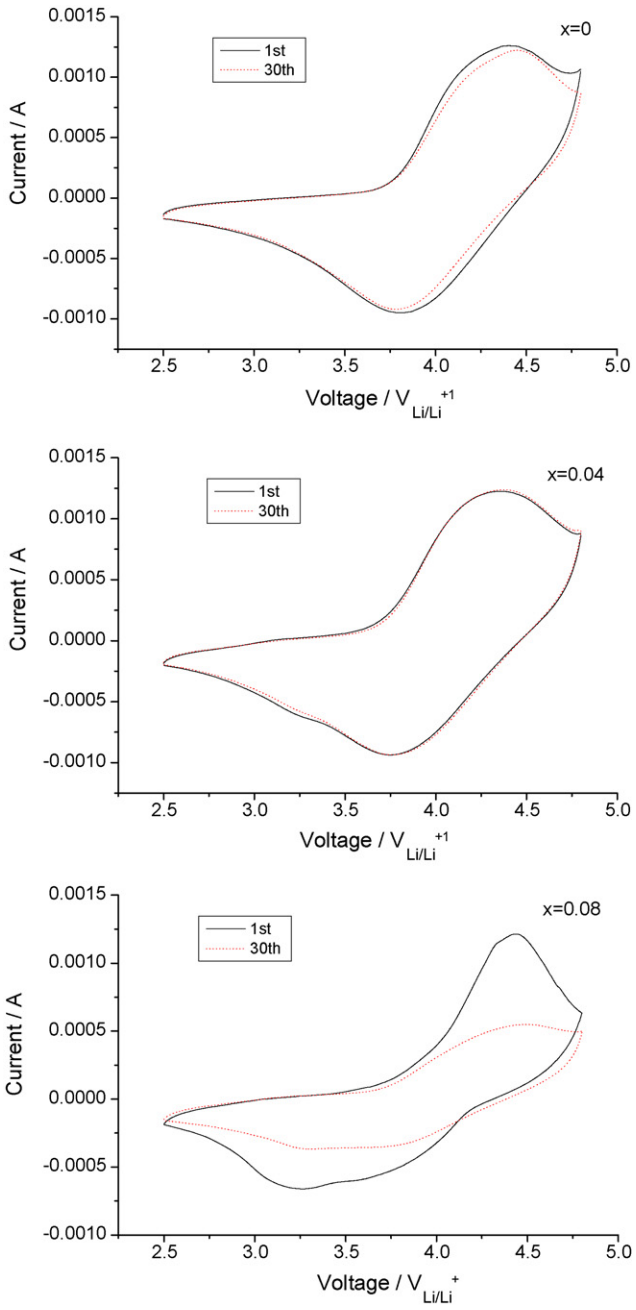

Fig. 5. Cyclic voltammogram of the $Li/Li[Li_{0.2}Ni_{0.2-x/2}Mn_{0.6-x/2}Cr_x]O_2$ ($x = 0$, 0.04, 0.08) cells in the 2.5–4.8 V range at the scan rate of 1 mV s^{-1}.

4.3 V and cathodic peak at 3.8 V are due to the oxidation of Ni^{2+} to Ni^{4+} and the subsequent reduction of Ni^{4+} in the solid phase. It is noted that there was a small reduction peak near 3.2 V when $x = 0.04$, resulting from several reduction of Mn^{4+} into Mn^{3+} appeared in the samples. This observation indicates that Cr substitution induces some structural ordering or a reduction of stacking faults during the first Li de-intercalation [19,33]. For $x = 0.08$, the intensity of this peak is greater than that of the peak at about 3.8 V. It is suggested that several structural phase transitions in the host lattice may happen by over much Cr doping, which may result in the deterioration of electrochemical performances.

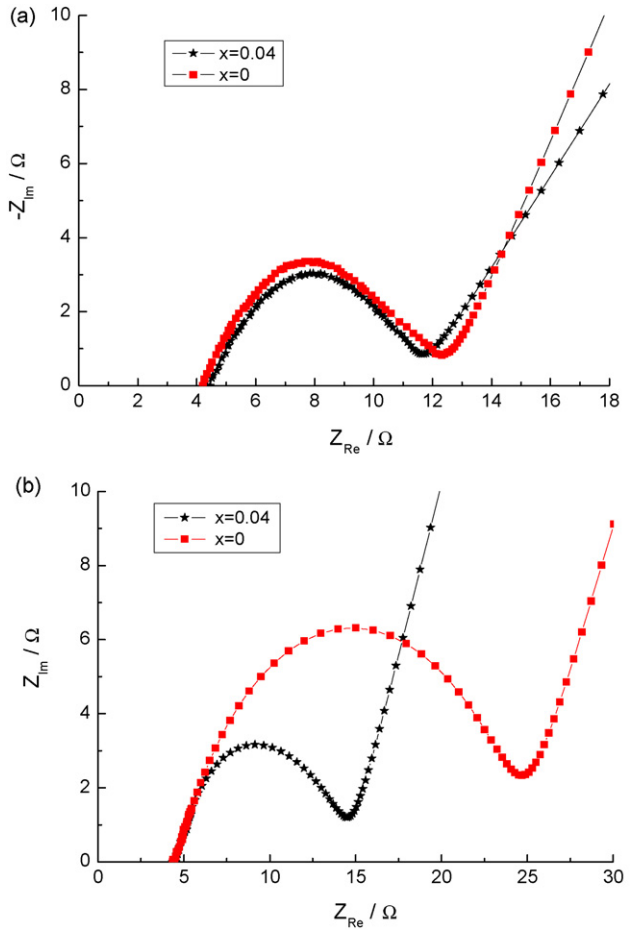

Fig. 6. Impedance spectra of $Li[Li_{0.2}Ni_{0.2-x/2}Mn_{0.6-x/2}Cr_x]O_2$ ($x=0$, 0.04) cells at: (a) charged to 4.8 V and (b) discharged to 2.5 V after 50 cycles.

As can be seen clearly from Fig. 5a, with cycling, the CV peaks became less sharp and the polarization (voltage difference between the charge and discharge curves) increased with increasing cycle number. Moreover, the peaks current for the cycled electrode was lower than that for the fresh one, it means that the structural degradation of the electrode leads to a capacity fading. On the contrary, Fig. 5b illustrates well the reversibility of the material with $x=0.04$ upon de-intercalation and intercalation of lithium-ions over the potential range, the polarization effect is very small compared to the material with $x=0$, and the negligible decrease in peak height with cycling is in agreement with the quite small loss in capacity shown by the cycling performance presented in Table 2. For $x=0.08$, the peak became broad and the area under the peak deceased after 30 cycles, this voltammogram clearly reveals a large capacity fading of electrode.

For the $Li[Li_{0.2}Ni_{0.2-x/2}Mn_{0.6-x/2}Cr_x]O_2$ ($x=0$, 0.04) electrodes, ac impedance was measured to explore the difference in cycling characteristics. Fig. 6a and b illustrates the impedance spectra at fully charged and discharged state, respectively, at the 50th cycle. The impedance spectra consist of two semicircles in high and intermediate-frequency ranges and a line inclined at constant angle to the real axis in the low-frequency range. The two semicircles in the higher and intermediate frequency range might due to the contact resistance at the composite cathode and the charge transfer reaction at the interface of the cathode/electrolyte, and the inclined line in the lower frequency range is attributed to Warburg impedance that is associated with lithium ion diffusion through the cathode. As observed in Fig. 6b, the resistance of $Li[Li_{0.2}Ni_{0.2-x/2}Mn_{0.6-x/2}Cr_x]O_2$ with $x=0.04$ is much smaller than that of the undoped electrode. The difference of R_{ct} between charge and discharge was about 3 Ω for the Cr-doped electrode, whereas that of undoped one was 13 Ω. The great decrease of R_{ct} between charge and discharge is considered to be the effect of Cr, resulting in the improvement of the electric conductivity. This agrees well with the result in Fig. 3.

4. Conclusion

$Li[Li_{0.2}Ni_{0.2-x/2}Mn_{0.6-x/2}Cr_x]O_2$ ($x=0$, 0.02, 0.04, 0.06, 0.08) materials have been synthesized using solid-state pyrolysis method. The effect of chromium doping on the structure and electrochemistry was investigated. By increasing Cr-doping amount in $Li[Li_{0.2}Ni_{0.2-x/2}Mn_{0.6-x/2}Cr_x]O_2$, the calculated lattice based on *R*-3*m* space group decreased, and the ratio of *c*/*a* increased monotonously. Furthermore, the gradual increase in the *c*/*a* ratio means that Cr doping resulted in much layer-like structure. These indicated that Ni and Mn were well replaced by Cr, and the solid solution was successfully formed. From the electrochemical charge–discharge and rate capability tests, the difference in various amount of doping chromium resulted in different morphology (shape and particle size) and thereby different initial discharge capacity and the rate capability. Among those electrodes, simple with $x=0.08$ shows the highest first discharge capacity of 261 mAh g^{-1}, but it also represented an accelerated deterioration with cycling while the Cr-doped electrode with low Cr content showed excellent cycling behavior especially at higher current density. From ac impedance measurements, it was clearly found that Cr replacement brought about decrease in resistance during cycling. It is considered that the higher capacity and superior rate capability of Cr-doping sample, especially for the sample $Li[Li_{0.2}Ni_{0.2-x/2}Mn_{0.6-x/2}Cr_x]O_2$ with $x=0.04$, would be ascribed from the reduced resistance of the electrode during cycling. Therefore, Cr-doping was potentially attractive to electrochemical application since Cr-doped has advantages such as higher intercalation voltage, higher rate capability, and lower cost. However, the method also has some disadvantages such as repeatability of the whole examination is not as good as some other methods [34–37] because the raw materials cannot be blend thoroughly well-proportioned by using mortar and pestle. Further studies to optimize composition and processing conditions are necessary to achieve improved properties; such studies are being carried out for high-power and high energy applications.

Acknowledgements

This work was supported by NSFC (200673062), TSTC (06YFJMJC04900) and 973 program (2002CB 211800).

References

[1] T. Ohzuku, Y. Makimura, Chem. Lett. (2001) 642.
[2] E. Rossen, C.D.W. Jones, J.R. Dahn, Solid State Ionics 57 (1992) 311.
[3] Q. Zhong, A. Bonakdarpour, M. Zhang, Y. Gao, J.R. Dahn, J. Electrochem. Soc. 144 (1997) 205.
[4] B.J. Neudecker, R.A. Zuhr, B.S. Kwak, J.B. Bates, J.D. Roberson, J. Electrochem. Soc. 145 (1998) 4148.
[5] M. Yoshio, Y. Todorov, K. Yamato, H. Noguchi, J. Itoh, M. Okada, T. Mouri, J. Power Sources 74 (1998) 46.
[6] J.M. Paulsen, C.L. Thomas, J.R. Dahn, J. Electrochem. Soc. 147 (2000) 861.
[7] Y. Grincourt, C. Stoery, I.J. Davidson, J. Power Sources 97–98 (2001) 711.
[8] Z. Lu, J.R. Dahn, J. Electrochem. Soc. 149 (2002) A815.
[9] J.-H. Kim, C.S. Yoon, Y.-K. Sun, J. Electrochem. Soc. 150 (2003) A538.
[10] A.R. Armstrong, P.G. Bruce, Nature 381 (1996) 499.
[11] Y. Shao-Horn, S.A. Hackeray, J. Electrochem. Soc. 146 (1999) 2404.
[12] B. Ammundsen, J. Paulsen, Adv. Mater. 13 (2001) 943.
[13] B. Ammundsen, J. Desilvestro, R. Steiner, P. Pickering, Proceedings of the 10th International Meeting on Lithium Batteries, Como, Italy, May 28–June 2, 2000.
[14] T. Ohzuku, Y. Makimura, Chem. Lett. (2001) 744.
[15] K. Numata, C. Sakaki, S. Yamanaka, Solid State Ionics 117 (1999) 257.
[16] L.H. Yu, Y.L. Cao, H.X. Yang, X.P. Ai, Y.Y. Ren, Mater. Chem. Phys. 88 (2004) 353.
[17] Z. Lu, D.D. MacNeil, J.R. Dahn, Electrochem. Solid State Lett. (2001) A191.
[18] J.-H. Kim, C.W. Park, Y.-K. Sun, Solid State Ionics 164 (2003) 43.
[19] Z. Lu, L.Y. Beaulieu, R.A. Donaberger, C.L. Thomas, J.R. Dahn, J. Electrochem. Soc. 149 (2002) A778.
[20] Z. Lu, J.R. Dahn, J. Electrochem. Soc. 150 (2003) A1044.
[21] C. Sigala, D. Guyomard, A. Verbaere, Y. Piffard, M. Tournoux, Solid State Ionics 81 (1995) 167.
[22] D. Zhang, B.N. Popov, R.E. White, J. Power Sources 76 (1998) 81.
[23] E. Iwata, K. Takahashi, T. Maeda, T. Mouri, J. Power Sources 81/82 (1999) 430.
[24] R. Thirunakaran, K.-T. Kim, Y.-M. Kang, C.-Y. Seo, J. Y-Lee, J. Power Sources 137 (2004) 100.
[25] J. Cho, B. Park, J. Power Sources 92 (2001) 35.
[26] C.W. Wang, X.L. Ma, J.L. Cheng, L.Q. Zhou, J.T. Sun, Y.H. Zhou, Solid State Ionics 177 (2006) 1027.
[27] S.H. Na, H.S. Kim, S.I. Moon, Solid State Ionics 176 (2005) 313.
[28] J.G. uo, L.F. Jiao, H.T. Yuan, H.X. Li, M. Zhang, Y.M. Wang, Electrochim. Acta 51 (2006) 3731.
[29] Y.-J. Kang, J.-H. Kim, S.-W. Lee, Y.-K. Sun, Electrochim. Acta 50 (2005) 4784.
[30] Y.C. Sun, Y.G. Xia, H. Noguchib, Electrochem. Solid State Lett. (2005) A637.
[31] K.M. Shaju, G.V. Subba Rao, B.V.R. Chowdari, Electrochim. Acta 48 (2003) 1505.
[32] S.H. Kang, K. Amine, J. Power Sources 119–121 (2003) 150.
[33] K.M. Shaju, G.V. Subba Rao, B.V.R. Chowdari, J. Electrochem. Soc. 150 (2003) A1.
[34] D.C. Li, T. Muta, L.Q. Zhang, M. Yoshio, H. Noguchi, J. Power Sources 132 (2004) 150.
[35] T.H. Cho, S.M. Park, M. Yoshio, T. Hirai, Y. Hideshima, J. Power Sources 142 (2005) 306.
[36] J.M. Kim, H.T. Chung, Electrochim. Acta 49 (2004) 3573.
[37] S. Gopukumar, K.Y. Chung, K.B. Kim, Electrochim. Acta 49 (2004) 803.